Large, J. P., R. Martin, and M. Niclause, "La pyrolyse du butane normal à faible advancement," *Bull. Soc. Chim. France*, 3, 961 (1972).
Paul, R. E., and L. F. Marek, "The Pyrolysis of i.Butane," *Ind. Eng. Chem.*, 26, 454 (1934).
Sagert, N. H., and K. J. Laidler, "Kinetics and Mechanisms of the Pyrolysis of n.Butane," *Can. J. Chem.*, 41, 883 (1963).
Torok, J., and S. Sandler, "Kinetics of the Pyrolysis of n.Butane," *ibid.*, 47, 2707 (1969).
Van Damme, P., S. Narayanan, and G. F. Froment, "Thermal Cracking of Propane and Propane-Propylene Mixtures: Pilot Plant Versus Industrial Data," *AIChE J.*, 21, 1065 (1975).

*Manuscript received July 6 and accepted September 28, 1976.*

# Fluid Vortices and Mass Transfer in a Curved Channel Artificial Membrane Lung

**KEITH GILROY**
**ELSPETH BRIGHTON**
**and**
**JOHN D. S. GAYLOR**

**Bioengineering Unit, University of Strathclyde**
**Glasgow, G4 ONW, Scotland**

Experimental assessment of theory on the convective dispersion of blood gases by vortices in a curved channel exchanger has demonstrated the impracticality of the proposed design. A nonlinear stability analysis of the fluid dynamics provided an amplitude factor an order of magnitude less than that previously assumed for the system secondary circulations.

## SCOPE

For short periods (for example, cardiac surgery), the respiratory function of the natural lung is adequately performed by exchangers in which the blood is in direct contact with the ventilating gas. However, for extended respiratory support, it is necessary to interpose a gas permeable membrane between the blood and gas phases in order to reduce blood trauma caused by direct contact systems (Lee et al., 1961). In the majority of membrane lungs (oxygenators), the blood flow is rectilinear laminar within parallel plate or tubular conduits, and with present membranes the oxygen and carbon dioxide transfers are limited by diffusion through the concentration boundary layer adjacent to the membrane (Mockros and Weissman, 1971). To take advantage of high gas exchange rates offered by ultrathin silicone rubber and hydrophobic microporous membrane technology, and to create compact, economic, and simple oxygenators, development has centered on reducing the fluid phase diffusional resistance by decreasing boundary-layer thickness or generating convective mixing in the blood. These processes may be accomplished by passive or active means. Passive systems utilize the energy of the blood flow coupled with conduit geometry to create mixing, for example, secondary flows in coiled tubes, eddy flows due to surface perturbations and screens (Drinker, 1972). In active units, mixing is generated by external energy, for example, oscillation of curved tubes (Melrose et al., 1972) or toroidal chambers (Drinker, 1972), rotating disks (Hill et al., 1974), rotating cylinders (Smeby and Gaylor, 1974), and flow pulsation across grooved walls (Bellhouse et al., 1973). Generally passive methods are favored owing to ease of operation, simple construction, and the lower blood trauma produced.

Correspondence concerning this paper should be addressed to John D. S. Gaylor. Elspeth Brighton is at the University of Cambridge, Cambridge, England.

An exchanger of the passive type has been theoretically analyzed by Chang and Mockros (1971). The system is based on flow between concentric circular cylindrical membranes, driven by a pressure gradient perpendicular to the cylinder axes. Vortices generated by the centrifugal forces, above a critical blood flow rate, were predicted to give a very high oxygenation efficiency such that the channel length required for a 25% increase in hemoglobin oxygen saturation would be less than 1/5 000 of that required with laminar rectilinear flow. Because of the apparent promise offered by the above geometry and in the absence of relevant experimental work, an investigation into the potential of the system as a blood gas exchanger was undertaken. Studies involved verification of the vortices by flow visualization and measurement of oxygen transfer to water and to blood in a model membrane oxygenator.

## CONCLUSIONS AND SIGNIFICANCE

The experiments have shown that although vortices are generated in the proposed system as predicted, they provide no noticeable increase in mass transfer efficiency for either blood or water over that for rectilinear laminar flow.

A nonlinear analysis of the fluid dynamics has provided an amplitude factor for these secondary flows an order of magnitude less than that predicted by Chang and Mockros. This is illustrated by a scale factor of 3.42 as opposed to a value of 50 used in their theory.

Extrapolation of the data indicates that optimization of the design could increase the amplitude of secondary flows by a factor of 2.55. However, the magnitude is still very small (0.69% of mean tangential velocity) and is unlikely to make a significant improvement in the oxygenation process.

The justification for this study was the apparent highly efficient mass transfer capability of the system, and since we have shown this premise to be false, further work on the device would be of little practical value, especially since curved tube oxygenators of at least comparable efficiency have already been investigated by others (Dorson et al., 1969).

### CURVED CHANNEL FLUID DYNAMICS: REVIEW

The stability of tangential fluid flow between concentric circular cylinders under the action of a pressure gradient was first examined by Dean in 1928 and subsequently by Reid (1958) and Hammerlin (1958). Experimental verification of the main hypotheses of these investigators was reported by Brewster et al. (1959).

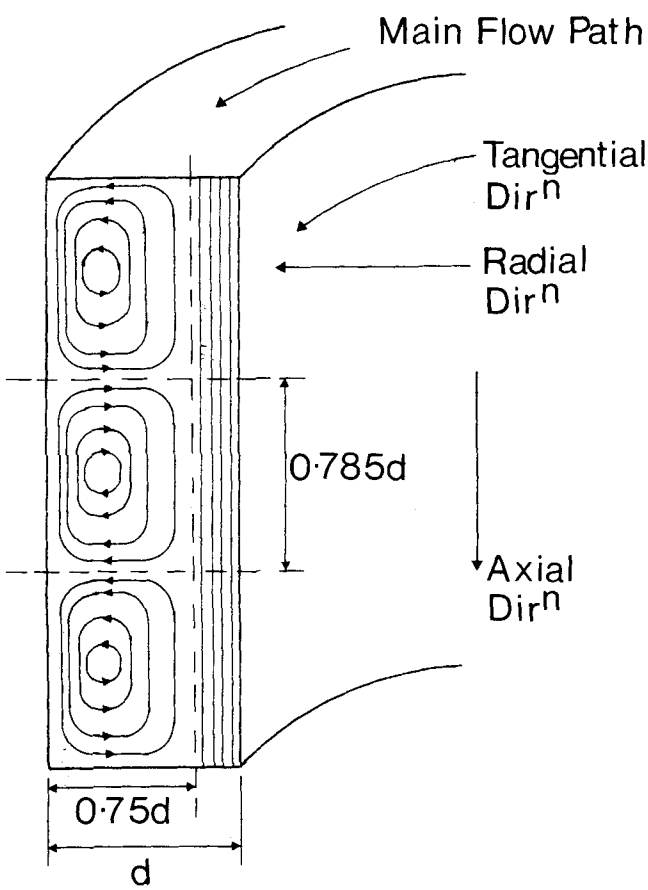


Fig. 1. Curved channel vortices at critical Dean number.

Owing to the centrifugal force field set up as fluid travels around a curved channel of rectangular cross section, the liquid in the central core is pushed towards the outer wall. This creates a transverse pressure gradient (that is, in the radial direction) which drives the fluid back towards the inner wall. At a critical flow rate, defined by the Dean number, a series of asymmetric counterrotating vortices is set up in a pattern repeated periodically in the axial direction. Providing that the inner radius of the channel is much greater than the gap width, the instability occurs when

$$Dn = Re\sqrt{\frac{d}{R_i}} \simeq 36$$

A schematic of the vortices in a plane along the cylinder axis is shown in Figure 1.

For a given radius of curvature, the centrifugal force is proportional to the square of the tangential velocity and

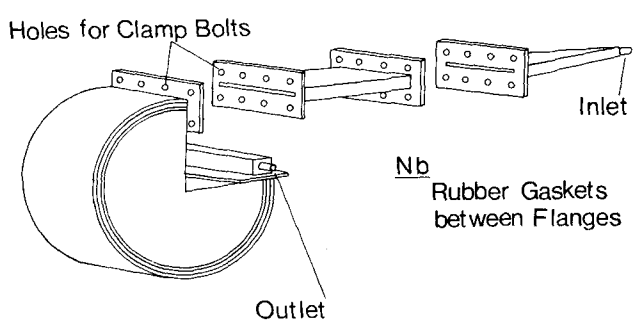


Fig. 2. Flow visualization model 1.

acts in a direction perpendicular to the main flow (Cheng and Akiyama, 1970). As the Dean number increases, the centers of the vortices shift towards the outer cylinder while the maximum secondary velocity decreases relative to the main flow.

As a result of his experiments on the initial growth of the disturbance, Brewster has postulated that the asymmetric vortex motion has its center some point in the channel defined by $\delta$ (where $\delta$ = width of unstable region), and each vortex near its center has almost circular streamlines in an axial plane. The preferred half wavelength of each vortex is approximately 1.58 in the radial direction. Now $\delta/d = 0.5$ (Brewster et al., 1959) in this case, and therefore the vortex depth = $0.75\ d$. This would suggest the existence of a layer of purely streamline fluid ($0.25d$) adjacent to the inner cylinder, at the critical Dean number, which is not indicated in Reid's analysis. However, Brewster's results do agree fairly well with Reid on the wavelength of the vortices in the axial plane at $Dn \simeq 36$. Reid calculated a wavelength of $1.57d$, whereas Brewster gives $(1.31 \pm 0.25)d$. From Reid's value, the width of each vortex = $0.785d$ as shown in Figure 1.

In order to solve the convective diffusion equations as a prerequisite to designing a blood oxygenator, based on the principle outlined above, knowledge of the amplitude of the secondary flow vortices and of the influence of increasing Dean number is required. To do this it is necessary to consider a nonlinear treatment of the stability problem. Because of the lack of a nonlinear stability analysis in the literature, Chang and Mockros (1971) were obliged to estimate the amplitude of the secondary circulation by analogy with Stuart's (1958) analysis of Couette flow. The validity of this estimation together with possible alternatives will be considered later.

## EXPERIMENTAL

### Flow Visualization

The main aims of the flow visualization study were to verify the existence of the secondary circulations, to determine wavelength variation with Dean number, to examine the effects of pulsatile flow and reduction of channel width on the vortices, and to study the influence of fluid viscosity and model orientation on the flow.

#### *Flow Model Design*

To ensure the validity of application of flow studies to oxygenator design, flow models were constructed with dimensions which would produce practical artificial lungs if this theory (Chang and Mockros, 1971) proved correct.

Flow model 1 was built with the following dimensions:

$$R_i = 6.98 \times 10^{-2}\ \text{m}$$

$$d = 3.18 \times 10^{-3}\ \text{m}$$

$$Z = 0.1\ \text{m}$$

This gives a radius to gap ratio of 22 and a width to gap ratio $Z/d$ of 31.4, which are comparable with Brewster's values ($R_i = 12d$, $Z = 35d$), to ensure agreement with

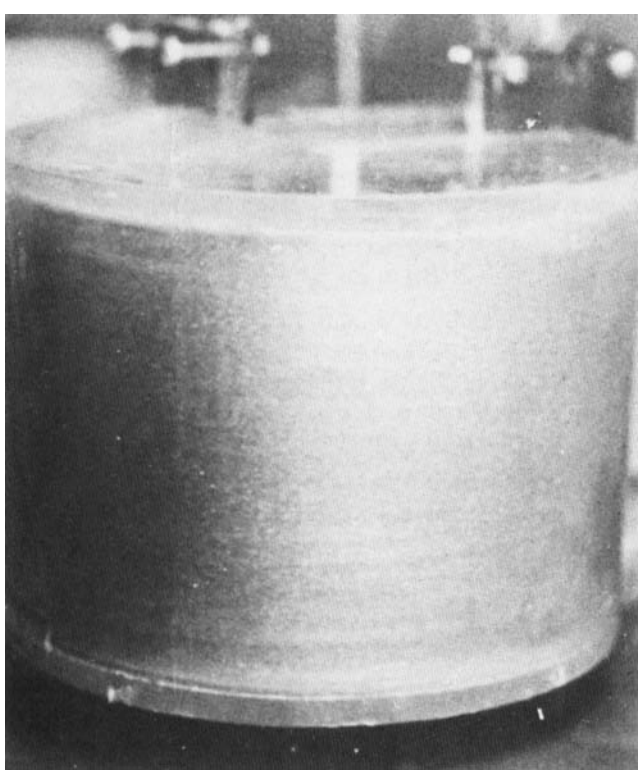

Fig. 3. Laminar flow ($11.67 \times 10^{-6}$ m$^3$/s) $Dn = 31$, $Re = 144.9$.

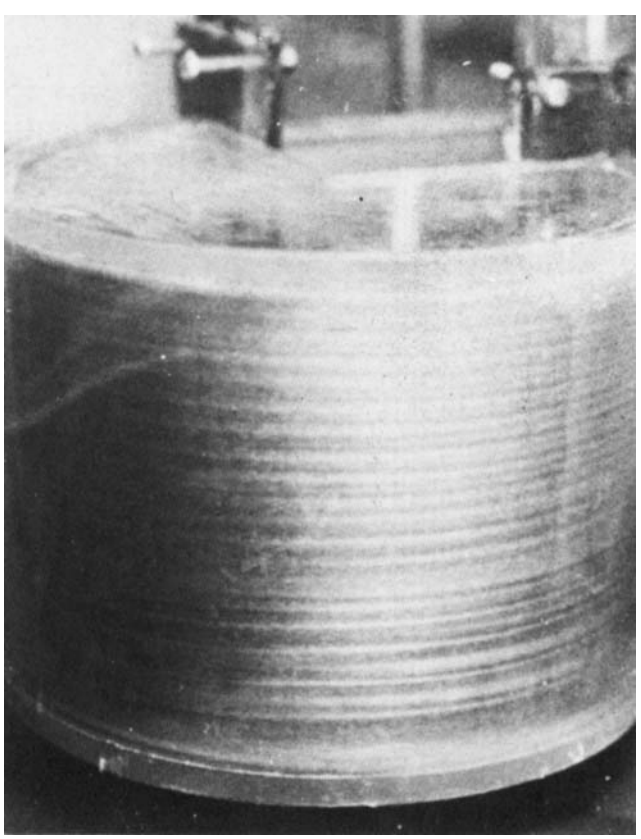

Fig. 4. Stable parallel vortices ($16.67 \times 10^{-6}$ m$^3$/s) $Dn = 44$, $Re = 207.0$.

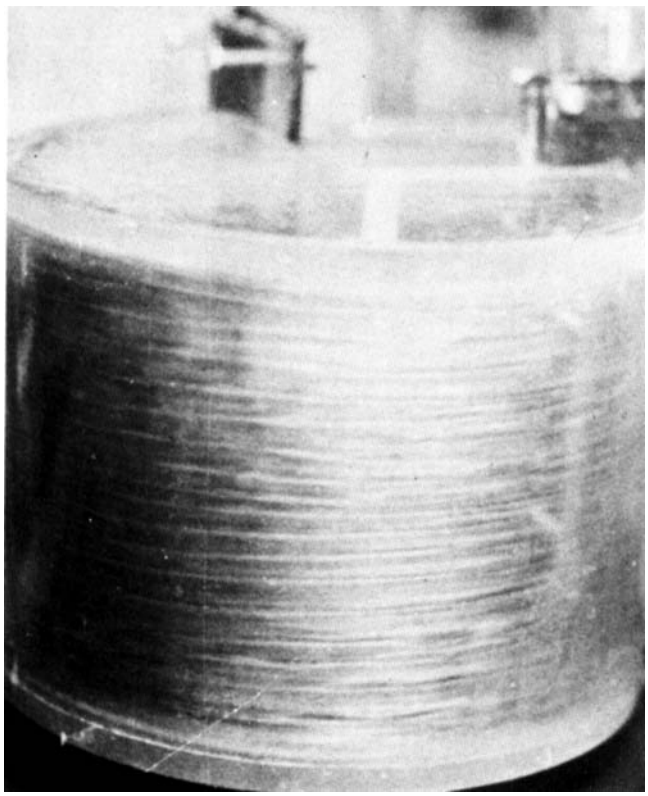

Fig. 5. Longitudinal waves ($33.33 \times 10^{-6}$ m$^3$/s) $Dn = 88$, $Re = 414.0$.

the fluid dynamical theory and effectively eliminate side wall effects. The dimensions give an oxygenator which would theoretically have a fluid limited channel requirement (75 to 100% saturation) of approximately $8 \times 10^{-2}$ m, while the available length is 0.44 m, neglecting obstructions due to manifolding and any entrance effects. With $Dn = 40$, the wall shear rate is $247 s^{-1}$ which is in excess of the minimum value ($200 s^{-1}$) required for blood to exhibit Newtonian behavior (Palmer, 1968).

To achieve undisturbed planar flow at entry to the curved channel, a diffuser shaped inlet manifold was designed to promote uniform distribution across the channel. The exit manifold consisted simply of a collecting channel which discharged fluid in the axial direction. The whole system was made of acrylics and assembled as shown in Figure 2.

Flow model 2 was designed to simulate the performance of a prototype gas exchanger and as such was built to operate at 10% above the critical Dean number with a blood flow rate of $5 \times 10^{-5} m^3 s^{-1}$. This was simply a narrower version of flow model 1 with a width of $6 \times 10^{-2}$m and, in this case the manifolds were $1 \times 10^{-2}$m internal diameter acrylic tubes attached perpendicularly to the outer cylinder wall and separated by an acrylic barrier across the channel.

### *Method*

A circuit was set up to give either controlled constant head or pulsatile fluid flow (peristaltic pump) with thermostatic temperature regulation to within ±0.1°C and a volumetric flow variability of approximately 1% over the velocity range considered. In the pulsatile situation the flow rate was found to oscillate ± 1% about the mean value. Following the work of Coles (1965), a suspension of aluminum paint pigment (particles of the order of $10^{-5}$m in size) in water was used as the visualization medium. Pigment concentration was 2 kg m$^{-3}$ which, although is excess of that used by Coles, was found to have negligible effect on the viscosity of the supporting fluid.

| | Model 1 | Model 2 | Reid | Brewster |
|---|---|---|---|---|
| wavelength x $10^2$ m | 0·489 ± 0·034 | 0·424 ± 0·024 | 0·499 | 0·416 ± 0·040 |

Fig. 6. Vortex wavelength comparison.

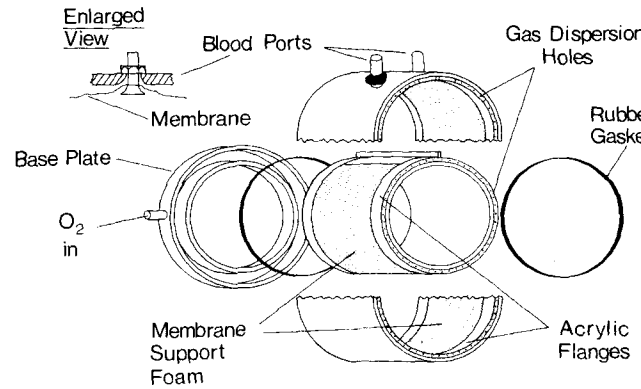


Fig. 7. Oxygenator design—exploded view.

### *Results of Flow Visualization*

The vortex motion was seen to occur as predicted at the critical Dean number of about 36, and the diffuser system gave good flow distribution at the inlet to model 1. Within the range of velocities studied, there was no variation in wavelength with velocity or position until Dean numbers in excess of 70 were created, at which point the flow broke into longitudinal waves. A typical range of flows are shown in the photographs (Figures 3, 4, and 5) from purely rectilinear laminar flow through stable parallel vortices to the longitudinal waves. A comparison of values of vortex wavelength with those determined theoretically by Reid and experimentally by Brewster shows fairly good agreement (Figure 6).

With the experimental variation kept in mind, the results from model 2 indicate no significant effect of reducing the channel width, and there was no apparent difference between pulsatile and nonpulsatile flow regimes with respect to vortex development. Similarly, the change in viscosity with glycerine solution ($4.5 \times 10^{-3}$ Ns/m$^2$, approximately that of normal human blood) had no effect on the Dean number at which the onset of secondary flows occurred, and there was also no measurable increase in pressure drop across the device at this point. By examination of the flow patterns in this model, it was observed that the vortices occurred almost immediately on entry, although they only attained stability after about 90 deg travel in the tangential direction. Orientation of flow model with axis vertical or horizontal did not affect the vortex characteristics.

These results indicate that a system based on model 2 should satisfactorily generate vortices above $Dn = 36$ when used with blood and a pulsatile pumping system. Although the manifolds are imperfect, their simplicity favor their use in a prototype oxygenator with further design pending verification of the theory. The predicted length requirement 0.08 m for full saturation at $5 \times 10^{-5} m^3 s^{-1}$ ($Dn = 40$) is much smaller than that available

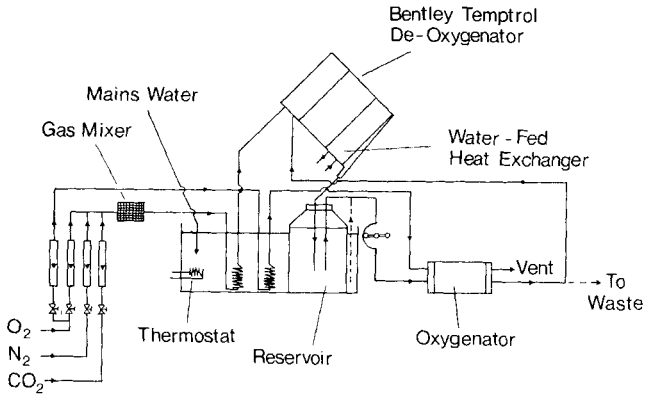


**Fig. 8. Flow circuit for oxygen transfer.**

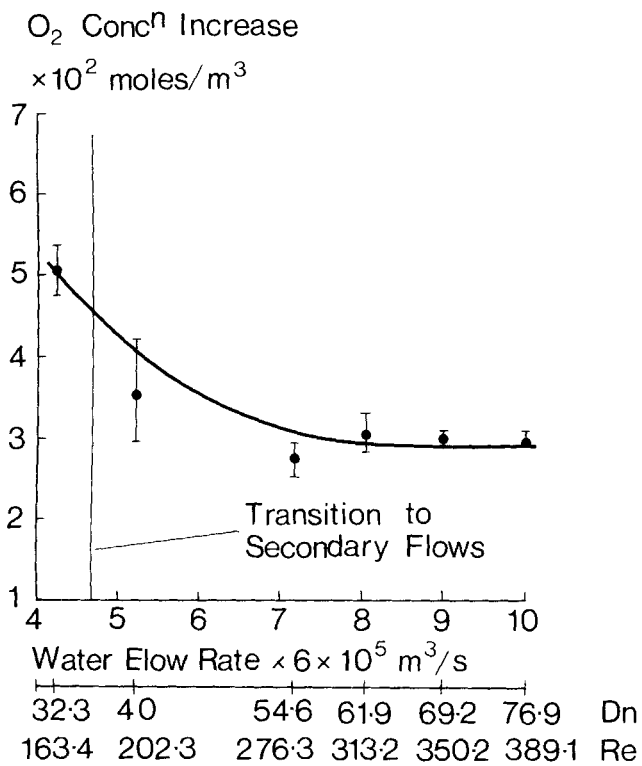


**Fig. 10. Oxygen concentration increase vs. water flow rate for 0.4 m channel oxygenator.**

(0.42 m) for a fluid limited oxygenation system, even allowing for development of the full vortex profile after entry.

The construction of a prototype blood oxygenator for mass transfer studies was therefore undertaken as follows.

### Mass Transfer Studies

*Oxygenator Design*

The oxygenator design was based on an acrylic concentric cylinder arrangement similar to that used in flow visualization model 2. A membrane support was provided by resin strengthened open-pore foam. The support was attached to the opposing surfaces of the inner and outer cylinders being flanked by acrylic flanges at the cylinder ends (Figure 7). The flanges served to duct ventilating gas (100% oxygen) to the foam by means of holes coaxial with the cylinders. A microporous polypropylene membrane (Celgard 2400, Celanese Plastics, Inc., $2.54 \times 10^{-5}$m thick) was bonded to the flange surfaces, thereby forming the fluid annulus. The channel ends were sealed

| $Q \times 10^5$ $m^3/s$ | Re | Dn | $PO_2 \times 10^{-2}$ $N/m^2$ | | $O_2$ sat$^n$% | |
|---|---|---|---|---|---|---|
| | | | in | out | in | out |
| 2·367 | 98·5 | 19·5 | 47·1 | 38·7 | 17·7 | 18·6 |
| | | | 36·5 | 35·9 | 14·9 | 14·4 |
| 3·200 | 133·2 | 26·3 | 44·5 | 47·2 | 22·5 | 22·4 |
| | | | 54·5 | 57·4 | 31·0 | 32·7 |
| 4·017 | 167·2 | 33·1 | 82·0 | 85·4 | 56·8 | 58·8 |
| | | | 92·9 | 94·4 | 67·6 | 68·1 |
| 4·433 | 184·5 | 36·5 | 79·3 | 78·8 | 52·3 | 51·8 |
| | | | 66·5 | 65·8 | 42·5 | 41·9 |
| 4·633 | 192·9 | 38·1 | 65·7 | 67·2 | 44·4 | 47·2 |
| | | | 84·0 | 84·4 | 62·6 | 62·8 |
| 4·850 | 201·9 | 39·9 | 76·4 | 74·1 | 56·0 | 53·3 |
| | | | 66·8 | 66·6 | 48·5 | 47·9 |
| 5·050 | 210·2 | 41·6 | 63·6 | 63·6 | 49·2 | 49·6 |
| | | | 65·2 | 67·2 | 59·8 | 62·0 |
| 5·167 | 215·1 | 42·5 | 78·5 | 74·8 | 63·4 | 61·2 |
| | | | 73·6 | 73·2 | - | - |
| Mean pH = 6·86 ( 6·70 - 7·02 ) | | | | | | |
| Mean Hb = 155 ( 152 - 158 ) $kg/m^3$ | | | | | | |

**Fig. 9. Experimental bovine blood oxygenation data.**

with rubber cord and silicone rubber compound. Fluid access to the annulus was provided by two stainless steel ports which mated with depressions in the outer cylinder inner surface. An acrylic barrier between the ports provided unidirectional flow in the annulus. Gas was distributed to the holes in the flanges via a ring shaped manifold which also served to accurately define the channel dimensions. Gas was allowed to vent freely to the atmosphere through holes in the top of the device.

The system provided the following channel dimensions:

$$d = 2.6 \times 10^{-3}\ \text{m}$$

$$R_i = 6.65 \times 10^{-2}\ \text{m}$$

$$Z = 5.7 \times 10^{-2}\ \text{m}$$

Effective channel length = 0.40 m

*Procedure, Oxygen Transfer to Blood*

The circuit shown in Figure 8 was set up to measure oxygen transfer in this oxygenator. Four liters of filtered heparinized cattle blood were maintained at 37 ± 0.1°C in a reservoir surrounded by a water bath. A peristaltic pump transferred blood from the reservoir to the oxygenator. It then passed to a Bentley Temptrol oxygenator from which it exited back to the reservoir. The Bentley unit served to deoxygenate the returning blood and to maintain its temperature by means of a built-in heat exchanger. By varying the proportion of nitrogen, oxygen, and carbon dioxide gases to the deoxygenator, oxygenator blood inlet conditions could be adjusted as required. An electrode system (ABC 1, Radiometer, Copenhagen) provided measurements of blood *p*H and oxygen and carbon dioxide partial pressures, while haemoglobin oxygen saturation and total haemoglobin concentration were obtained with the aid of an IL 182 Co-oximeter (Instrumentation Laboratories, Inc.).

*Procedure, Oxygen Transfer to Water*

As indicated by the dotted lines in Figure 8, water was fed directly from the thermostat tank to the oxygenator

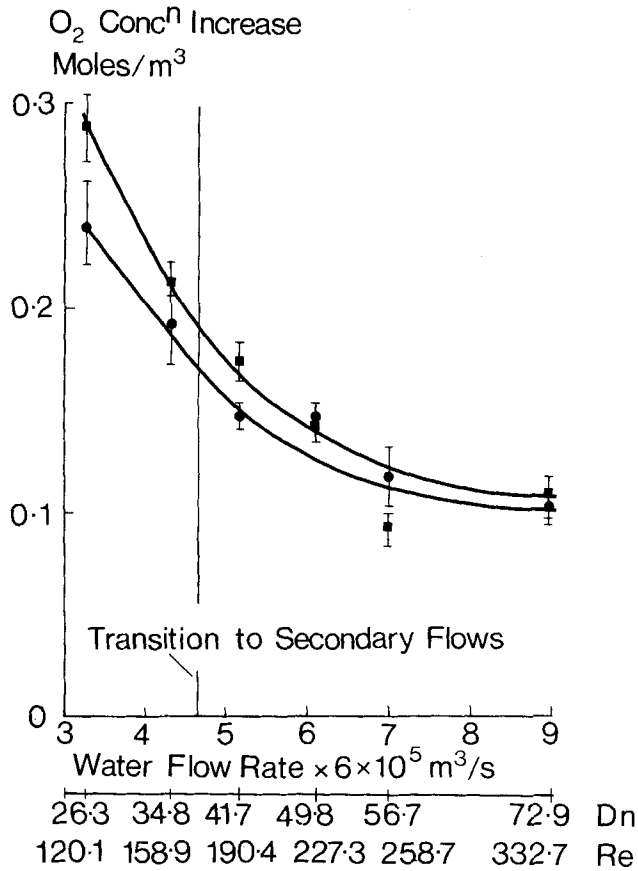


**Fig. 11. Oxygen concentration increase vs. water flow rate for helical oxygenator (2.0 m).**

and then discharged to waste. A continuous flow was maintained by feeding water to the tank from the mains supply, and oxygen was provided as before. Tests were undertaken for a range of flow rates spanning the critical Dean number, with oxygen partial pressures being measured by the Radiometer instrument.

## RESULTS OF MASS TRANSFER STUDIES

### Oxygen Transfer to Blood

The experimental data are presented in Figure 9 (NB: oxygen supply rate = $8.33 \times 10^{-5}m^3s^{-1}$, blood haematocrit = 45%, atmospheric pressure = $1.004 \times 10^5N/m^2$).

Examination of the saturation increase as a function of Dean number indicates no noticeable change upon generation of the secondary flows. In fact, the trend is disguised by the experimental error (of the order of 5%) in individual runs.

In order to ascertain whether or not secondary flows generated in this system do increase mass transfer, it was decided to perform water oxygenation tests by the method described above. Owing to the lower flow rates required to produce a given Dean number, more accurate data could be obtained. The results for these tests are given below.

### Oxygen Transfer to Water

Figure 10 shows oxygen concentration increase expressed as a function of Dean number, Reynolds number, and flow rate. The data again seem to confirm that the onset of vortices does not appreciably alter the mass transfer performance of the oxygenator.

As a further check on this phenomenon, it was decided to construct an oxygenator with a much greater channel length to produce a higher concentration difference between inlet and outlet.

This was achieved by the design of a helical arrangement, whereby a Celgard bag, 2 m in length, was wrapped around an elongated version of the inner cylinder of the previous device. A suitably lengthened outer cylinder was placed around this as before, and a similar gas dispersion system adopted. This oxygenator had the following dimensions:

$$d = 3.2 \times 10^{-3}\text{m}$$
$$R_i = 6.67 \times 10^{-2}\text{m}$$
$$Z = 6.0 \times 10^{-2}\text{m}$$
$$\text{length} = 2.0\text{ m}$$
$$\text{helix angle to horizontal} = 10\text{ deg.}$$

To verify that secondary flows did occur in this system, a flow visualization experiment was first undertaken utilizing the water/aluminium powder technique as previously described. By replacing the outer cylinder with a clear acrylic one, and by coating the bag with silicone grease to make it transparent, it was observed that vortices occurred at the critical Dean number and were of the same form as before. Smoke tests with this device demonstrated that adequate oxygen distribution was achieved throughout the channel length.

Data from two experiments with this oxygenator are presented in Figure 11 as a plot of concentration increase vs. Dean number, Reynolds number, and flow rate.

These graphs give comparable results to the previous tests, indicating no augmented oxygen transfer at onset of vortices.

## DISCUSSION

The experimental data indicate no vortex augmented mass transfer of the magnitude predicted by theory. Since the vortices have been shown to occur in models geometrically similar to the mass transfer apparatus, there are three other factors that may account of the discrepancy between experiment and theory. First, the oxygen transfer rate is limited by the membrane resistance. Second, the oxygen transfer rate is limited by the gas phase resistance. Last, the theoretical prediction is overoptimistic.

### Membrane Resistance

The oxygen permeability of the membrane Celgard 2400 used in this study is $1.042 \times 10^{-7}$ m³ (STP)-m thick/s-m²-atm (Gilroy, 1976). For the membrane area and average $PO_2$ driving force encountered in the blood experiments, the oxygen transfer rate, if the membrane were rate controlling, would be $1.7 \times 10^{-4}$m³ (STP)/s. The maximum oxygen transfer rate measured was $2.69 \times 10^{-7}$m³ (STP)/s. Thus, it is obvious that the membrane offers negligible resistance.

### Gas Phase Resistance

The membrane possesses a high water vapor transmission rate. Thus it is conceivable that a water layer would be formed in the gas side which would impede transport. By maintaining a high flow rate of heated ventilating gas, the formation of a water layer was prevented.

### Theoretical Prediction of Chang and Mockros (1971)

Using an I.C.L. 1904s computer, the fluid limited secondary flow program (Chang, 1969) was run with input data from the blood experiments with an inlet saturation of 49.2%. The resulting solution gave a saturation increase of 1.5% in a channel length of $1.3 \times 10^{-2}$m. Unfortunately, the program could not be run for the necessary num-

ber of steps because of the excessive computer time involved. Nevertheless, since the calculated oxygen saturation increase for about one thirtieth of the channel is of the same order of magnitude as the experimental values for the whole channel, the theory obviously grossly overestimates the strength of the secondary flows generated in this system. In fact, calculation of the theoretical concentration increase with water in laminar flow, from their unperturbed flow program, yields the result that there is no significant difference in mass transfer between flows with or without secondary circulation in the oxygenators described here.

The most apparent source of error in the theory occurs in the assumption of an amplitude for the disturbances by analogy with Couette flow. It was necessary for Chang and Mockros to estimate this quantity, since there was no suitable analysis available in the literature.

To provide a more appropriate amplitude factor, we performed a nonlinear stability analysis using the method of Stuart (1958). We investigated the possibility of an equilibrium state in which the rate of transfer of energy from the mean flow to the disturbance balances precisely the rate of viscous dissipation of the energy of the disturbance. In such an equilibrium state, the disturbance will have a definite finite amplitude, and the mean flow will be distorted from the original laminar flow.

Following Stuart, we assumed that the dominant nonlinear interaction is between the mean flow and the first harmonic component of the disturbance, where the latter is assumed to be similar in shape to that given by the linear theory but multiplied by an amplitude factor $a$. We restricted consideration to narrow gap width ($d << R_i$) and used the results of Reid (1958) for the linear case. Carrying out this procedure, we got an energy equation

$$\text{(constant)}.\frac{da^2}{dt} = a^2 \times 41.14 \times 10^{-4} - \frac{a^4 R_i}{36d} 48.35 \times 10^{-6} - \frac{a^2\, 1\,549}{\lambda^2 T} \quad (1)$$

where

$$\lambda = 3.98, \mathrm{T} = \frac{18(Re)^2 d}{R_i}$$

Neglecting the term in $a^4$, the Reynolds stress term, we see that the critical Taylor number is given by

$$\lambda^2 Tc = 37.65 \times 10^4$$

that is $Dn = 36.34$, which agrees satisfactorily, in view of the approximations inherent in the method, with the value of 35.94 given by Candrasekhar (1961).

We are interested in the equilibrium state $da^2/dt = 0$. The equilibrium amplitude is given by

$$a_e^2 = 3\,063 \frac{d}{R_i}\left(1 - \frac{Tc}{T}\right) \quad (2)$$

The amplitude factor $\alpha$ and associated quantity $\beta$ of Chang and Mockros are given by

$$\alpha = \frac{\beta}{Re}\sqrt{1 - \frac{Tc}{T}} = \frac{a_e \nu}{6\lambda} \quad (3)$$

and

$$\beta = \frac{\nu}{\lambda 6}\sqrt{3\,063}\, Dn \quad (4)$$

$\beta$ has the dimensions of viscosity and will be given in centimeter-gram-second units for ease of comparison. (Note: The complete mathematical analysis is given in the Supplement to this paper.)

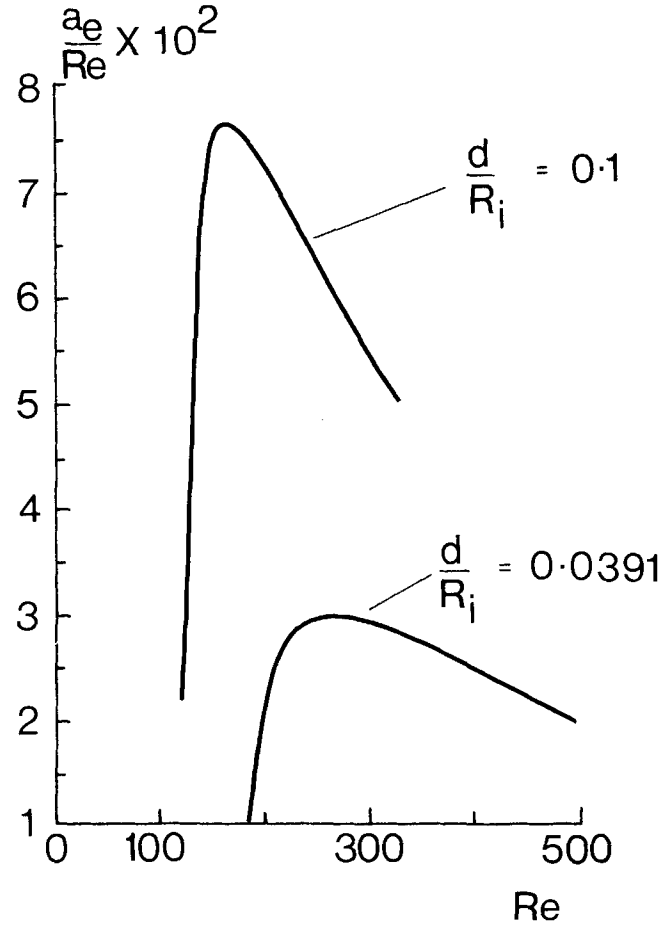


Fig. 12. Relative vortex amplitude vs. Reynolds number.

This shows that in fact $\beta$ is not a constant as suggested by Chang and Mockros but depends on the fluid properties, system geometry, and flow rate. A comparison with the example cited in their paper (1971) for $T = 1.05Tc$, $d/R_i = 0.1$, and $\nu = 0.04$ cm$^2$ s$^{-1}$ gives $\beta = 3.42$ cm$^2$ s$^{-1}$. This compares with their estimated value of 50 for this constant.

From the size of this result it is not surprising, therefore, that these secondary flows, much weaker than Chang and Mockros had supposed, do not appreciably enhance mass transfer.

Now, Equation (2) can be used to examine possible means of improving the relative vortex strength in this system if it is rewritten as

$$\frac{a_e}{Re} = \frac{\sqrt{3\,063}}{Re}\sqrt{\frac{d}{R_i}}\left(1 - \frac{Tc}{T}\right)^{1/2} \quad (5)$$

since $a_e/Re$ is proportional to $V_x/V_m$ for a given geometry and fluid.

A plot of Equation (5) against Reynolds number (Figure 12) spanning the range of experimental values in Figure 9 indicates that the maximum relative vortex amplitude occurs at about $Re = 250$. Although the maximum Reynolds number used in the blood experiments reported here was 215, the increased amplitude achieved by using 250 can be estimated as less than 2%. In fact, Reynolds numbers of up to 389 were used in the water oxygenation tests with this device, and no mass transfer augmentation was

observed at these high levels (Figure 10).

This shows, then, that significant improvement in oxygenation efficiency could not be achieved by the use of higher flow rates.

Equation (5) also suggests that an increase in $d/R_i$ would be conducive to increased vortex amplitude. In the experimental blood oxygenator, a value of $d/R_i = 0.0391$ was used; however, it should be possible to increase this to about 0.1 while still remaining within the limits required by the analysis technique. To examine the effects of such an increase, $a_e/Re$ is shown plotted in Figure 12 for $d/R_i = 0.1$.

If one takes the two maxima corresponding approximately to $Re = 250$ and 160, these give secondary velocity components of 0.27% ($\beta = 4.58$) and 0.69% ($\beta = 4.69$) of $V_m$, respectively, for $d/R_i = 0.0391$ in the former case and $d/R_i = 0.1$ in the latter. Although the relative vortex velocity is increased, it is still very small, being an order of magnitude less than Chang's prediction of 7.4% from Equation (3) with $\beta = 50$.

The proposition that this vortex strength given by $\beta = 4.69$ provides little improvement of the oxygenation process is supported by some of the Chang and Mockros work. Using values of $\beta = 85$, 50, and 15, they calculated channel lengths required for 25% saturation increase with $d/R_i = 0.1$ and found that the mass transfer was highly dependent on the value of this parameter. As shown in their analysis, reducing the value of $\beta$ to 15 considerably increased the required channel length, and it is therefore likely that a further reduction to 4.69 would have a proportionately greater effect.


## ACKNOWLEDGMENT

This work was supported in part by funds awarded to Strathclyde University by the Science Research Council under grant number B/RG 73207.


### Greek Letters

- $\alpha$ = amplitude factor defined by Chang and Mockros
- $\beta$ = scale factor defined by Chang and Mockros
- $\lambda$ = dimensionless critical wave number for disturbance
- $\nu$ = kinematic viscosity
- $\delta$ = width of unstable region

## NOTATION

- $a$ = amplitude factor
- $a_e$ = equilibrium amplitude factor
- $d$ = gap width
- $Dn$ = Dean number
- Hb = haemoglobin concentration
- $PO_2$ = oxygen partial pressure
- $Q$ = blood flow rate
- $Re$ = Reynolds number $= V_m\, d/\nu$
- $R_i$ = radius of inner cylinder
- $t$ = time
- $T$ = Taylor number
- $Tc$ = critical Taylor number
- $V_m$ = mean velocity of unperturbed flow (tangential)
- $V_x$ = perturbed flow velocity component in radial direction
- $Z$ = channel width (axial direction)

## LITERATURE CITED


Bellhouse, B. J., F. H. Bellhouse, C. M. Curl, T. I. MacMillan, A. J. Gunning, E. M. Spratt, S. B. MacMurray, and J. M. Nelems, "A high efficiency membrane oxygenator and pulsatile pumping system, and its application to animal trials," *Trans. Am. Soc. Artif. Intern. Organs*, **19**, 72-79 (1973).

Brewster, D. B., P. Grosberg, and A. H. Nissan, "The stability of viscous flow between horizontal concentric cylinders," *Proc. Roy. Soc. (London)*, **A251**, 76-91 (1959).

Chandrasekhar, S., *Hydrodynamic and Hydromagnetic Stability*, Oxford Univ. Press, England (1961).

Chang, H.-K, "Gas Transport in Annular Oxygenators," Ph.D. thesis, Northwestern Univ., Evanston, Ill. (1969).

———, and L. F. Mockros, "Convective Dispersion of Blood Gases in Curved Channel Exchangers," *AIChE J.*, **17**, 541-549 (1971).

Cheng, K. C., and M. Akiyama, "Laminar forced Convection Heat Transfer in Curved Rectangular Channels," *Intern. J. Heat Mass Transfer*, **13**, 471-490 (1970).

Coles, D., "Transition in Circular Couette flow," *J. Fluid Mech.*, **21**, 385-425, (1965).

Dean, W. R., "Fluid motion in a curved channel," *Proc. Roy. Soc. (London)*, **A121**, 402-420 (1928).

Dorson, W. J., Jr., E. Baker, and M. L. Cohen, "A perfusion system for infants," *Trans. Am. Soc. Artif. Intern. Organs*, **15**, 155-160 (1969).

Drinker, P. A., "Progress in Membrane Oxygenator Design," *Anesthesiology*, **37**, 242-250 (1972).

Gilroy, K., Ph.D. thesis, Univ. Strathclyde, Glasgow, U.K. (1976).

Hammerlin, G., "Die Stabilität der Strömung in einem gekrümmten Kanal," *Arch. Rat. Mech. Anal.*, **1**, 212-224 (1958).

Hill, J. D., A. Latridis, R. O'Keefe, and S. Kitrilakis, "Technique for achieving high gas exchange rates in membrane oxygenation," *Trans. Am. Soc. Artif. Intern. Organs*, **20**, 249-252 (1974).

Lee, W. F., D. Krumhaar, G. Derry, D. Sachs, S. H. Lawrence, G. H. A. Clowes, and J. V. Maloney, "Comparison of the Effects of Membrane and Non-Membrane Oxygenators on the Biochemical and Biophysical Characteristics of Blood," *Surg. Forum*, **12**, 200-202 (1961).

Melrose, D. G., N. Burns, M. P. Singh, R. L. Elliot, R. Read, F. E. Williams, J. Becket, M. P. Lamb, and J. S. Adams, "Oscillating silicone membrane tubes: A new principle of extracorporeal respiration," *Biomed. Eng.*, **7**, 60-66 (1972).

Mockros, L. F., and M. H. Weissman, *Biomedical Engineering*, J. H. U. Brown, J. E. Jacobs, and L. Stark, ed., p. 325, F. A. Davis Co., Calif. (1971).

Palmer, A. A., Process First International Conference Haemorheology, A. L. Copley, ed., p. 391, Pergamon Press, London, England (1968).

Reid, W. H., "On the stability of viscous flow in a curved channel," *Proc. Roy. Soc. (London)*, **A244**, 186-198 (1958).

Smeby, L. C., and J. D. S. Gaylor, "Further Development of the Taylor—Vortex Membrane Oxygenator," *Proc. European. Soc. Artif. Organs*, **1**, 62-67 (1974).

Stuart, J. T., "On the nonlinear mechanics of hydrodynamic stability," *J. Fluid. Mech.*, **4**, 1-21 (1958).


## SUPPLEMENT: NONLINEAR STABILITY ANALYSIS—PRESSURE DRIVEN CURVED CHANNEL FLOW

We shall assume that the flow has rotational symmetry, is independent of $\theta$, and is confined to the region $R_i \leq r \leq R_o$. The unperturbed flow is thus of the form $[0, V(r), 0]$ with $V(R_i) = V(R_o) = 0$. Then, the Navier-Stokes equations and the equation of continuity are

$$\frac{\partial U}{\partial t} + \frac{U\partial U}{\partial r} + \frac{W\partial U}{\partial z} - \frac{V^2}{r} = -\frac{1}{\rho}\frac{\partial P}{\partial r} + \nu\left(\nabla^2 - \frac{1}{r^2}\right)U$$

$$\frac{\partial V}{\partial t} + \frac{U\partial V}{\partial r} + \frac{W\partial V}{\partial z} + \frac{UV}{r} = -\frac{1}{\rho r}\frac{\partial P}{\partial \theta} + \nu\left(\nabla^2 - \frac{1}{r^2}\right)V$$

$$\frac{\partial W}{\partial t}+\frac{U\partial W}{\partial r}+\frac{W\partial W}{\partial z}=-\frac{1}{\rho}\frac{\partial P}{\partial z}+\nu\nabla^2 W$$

$$\frac{1}{r}\frac{\partial(rU)}{\partial r}+\frac{\partial W}{\partial z}=0$$

where $$\nabla^2=\frac{\partial^2}{\partial r^2}+\frac{1}{r}\frac{\partial}{\partial r}+\frac{\partial^2}{\partial z^2}$$

It is known from the work of Dean and others that the steady laminar flow is unstable when a parameter known as the Dean number exceeds a critical value. Since the flow which results from the instability is periodic with respect to $z$, it is convenient to take averages with respect to $z$, denoted by $-$.

Let us write the disturbed flow as $U = u'$, $V = \bar{v} + v'$, $W = w'$. In this treatment the disturbance flow has zero mean, and the mean flow is not necessarily the unperturbed flow. The mean motion equations become

$$\frac{1}{r}\frac{\partial}{\partial r}(\overline{ru'^2})-\frac{1}{r}(\overline{v'^2}+\bar{v}^2)=-\frac{1}{\rho}\frac{\partial P}{\partial r}$$

$$\frac{\partial\bar{v}}{\partial t}+\frac{1}{r^2}\frac{\partial}{\partial r}(r^2\overline{u'v'})=\nu\left(\frac{\partial^2}{\partial r^2}+\frac{1}{r}\frac{\partial}{\partial r}-\frac{1}{r^2}\right)\bar{v}-\frac{1}{\rho r}\frac{\partial P}{\partial\theta}$$

We may impose the condition that the overall pressure gradient remains constant:

$$\frac{P}{\rho}=k\theta+f(r)\quad\text{with } k \text{ constant.}$$

This differs from the assumption made by Mori and Uchida (1967) that the volume flow rate is constant and so the form of all subsequent results differs from theirs.

Then in a state of equilibrium with $\partial\bar{v}/\partial t = 0$ we have

$$\bar{v}=\frac{rk}{2\nu}\log(r/R_i)-R_o^2\left(r-\frac{R_i^2}{r}\right)\frac{k}{2\nu}\frac{1}{(R_o^2-R_i^2)}\log(R_o/R_i)+\frac{r}{\nu}\int_{R_i}^{r}\frac{\overline{u'v'}}{\eta}d\eta-\frac{R_o^2}{\nu(R_o^2-R_i^2)}\int_{R_i}^{R_o}\frac{\overline{u'v'}}{\eta}d\eta\cdot\left(r-\frac{R_i^2}{r}\right)$$

$$=V_o+V_R$$

where the zero velocity condition on the bounding cylinders $r = R_i$ and $R_o$ has been used.

If we subtract mean motion equations from the full equations we obtain equations for the disturbance velocities. We may then obtain the disturbance energy equation which is an exact consequence of the equations for an axisymmetric disturbance:

$$\frac{\partial}{\partial t}\int\int\rho\frac{1}{2}(u'^2+v'^2+w'^2)rdrdz=\int\int(-\rho\overline{u'v'})\left(\frac{d\bar{v}}{dr}-\frac{\bar{v}}{r}\right)rdrdz-\rho\nu\int\int(\xi'^2+\eta'^2+\zeta'^2)rdrdz$$

where

$$\xi'=-\frac{\partial v'}{\partial z},\quad\eta'=\frac{\partial u'}{\partial z}-\frac{\partial w'}{\partial r}\quad\text{and}\quad\zeta'=\frac{1\partial}{r\partial r}(rv')$$

Let us now expand the disturbance velocities as Fourier series in $z$ so that

$$u'=u_1(r,t)e^{i\gamma z}+u_2(r,t)e^{2i\gamma z}+\cdots\cdots+\tilde{u_1}(r,t)e^{-i\gamma z}+\tilde{u_2}(r,t)e^{-2i\gamma z}+\cdots\cdots$$

where $\sim$ denotes the complex conjugate and similar expressions are used for $v'$ and $w'$. Following Stuart we assume that the dominant non-linear interaction is between the mean flow and the first harmonic component of the disturbance $(u_1, v_1, w_1)$ where the latter is assumed to be similar in shape to that given by the linear theory but multiplied by an amplitude factor. Mori and Uchida make a different assumption here introducing two amplitude factors. It is this feature of their work that makes comparison with Chang and Mockros' estimate so difficult. Davey (1962) found that inclusion of the harmonic $2\gamma z$ made little difference to results for the case of rotating cylinders with narrow gap and this has been confirmed by later work (Stuart, 1971). Without a great deal of extra analysis, it is not possible to say whether this approximation is equally good in the present case.

If we now restrict to first harmonics $u' = u\cos\gamma z$, $v' = v\cos\gamma z$, and $w' = w\sin\gamma z$. Considering an equilibrium state with $\partial/\partial t = 0$ and performing the $z$ integration, we have, from the energy equation,

$$0=\int_{R_i}^{R_o}(-\rho uv)\left(\frac{d\bar{v}}{dr}-\frac{\bar{v}}{r}\right)rdr-\rho\nu\int_{R_i}^{R_o}r\left\{\gamma^2v^2+\left(\alpha u+\frac{dw}{dr}\right)^2+\left(\frac{dv}{dr}+\frac{v}{r}\right)^2\right\}dr$$

$$=I+J+K$$

where

$$I=\int_{R_i}^{R_o}(-\rho uv)\left(\frac{dV_o}{dr}-\frac{V_o}{r}\right)rdr-\rho\nu\int_{R_i}^{R_o}r\left(\gamma^2v^2+\frac{v^2}{r^2}+\frac{2v}{r}\frac{dv}{dr}+\left[\frac{dv}{dr}\right]^2\right)dr$$

$$J=\int_{R_i}^{R_o}(-\rho uv)\left(\frac{dV_R}{dr}-\frac{V_R}{r}\right)rdr$$

and

$$K=-\rho\nu\int_{R_i}^{R_o}r\left(\gamma u+\frac{dw}{dr}\right)^2dr$$

$I$ and $K$ are quadratic in the amplitude factor $a$, whereas $J$ is a multiple of $a^4$. To evaluate $I$ we need the result from the linear theory, given by Chandrasekhar (1961), that

$$u\left(\frac{dV_o}{dr}+\frac{V_o}{r}\right)=\nu\left(\frac{d^2}{dr^2}+\frac{1}{r}\frac{d}{dr}-\frac{1}{r^2}-\gamma^2\right)v$$

Then

$$I=\int_{R_o}^{R_o}\left\{2\rho uvV_o-\rho\nu\left(rv\frac{d^2v}{dr^2}+3v\frac{dv}{dr}+r\left[\frac{dv}{dr}\right]^2\right)\right\}dr$$

$$=\int_{R_i}^{R_o}\{2\rho uvV_o\}dr-\rho\nu\left[rv\frac{dv}{dr}+v^2\right]_{R_i}^{R_o}$$

$$=\int_{R_i}^{R_o}2\rho uvV_odr,\quad\text{since}\quad v=0\quad at\quad r=R_i,R_o$$

To proceed further we need explicit expressions for $u$, $v$, $w$. These are most conveniently taken from the work of Reid. So far the work applies to any gap width, but to utilize Reid's solution we must restrict consideration to narrow gap width, that is, $d = R_o - R_i << R_i$, and we now retain only leading terms in $d/R_i$.

Let

$$V_m=-\frac{d^2k}{12\nu R_i}>0\quad\text{because}\quad k<0.$$

Then, if we define $y$ by $r = R_i + d(y + \frac{1}{2})$ we have $V_o = 6V_m(\frac{1}{4} - y^2)$ and a suitable nondimensionalization is

$$v = -V_m a S(y),\ u = -\frac{\nu P(y)}{6d}a,\quad \gamma = \frac{\lambda}{d}$$

We define

$$Re = \frac{V_m d}{\nu} = -\frac{kd^3}{12\nu^2 R_i}$$

and

$$T = 18\frac{(Re)^2 d}{R_i}$$

Continuity gives

$$w = -\frac{1}{\gamma}\frac{du}{dr}$$

Reid gives the first approximation to the solution as

$$P = C_1(y) + B_1 S_1(y)$$

$$S = a_1\frac{\sinh\lambda y}{\sinh \tfrac{1}{2}\lambda} - \frac{2y}{\lambda_1^4 - \lambda^4}(\lambda^2 C_1 + C_1'') + \frac{4}{(\lambda_1^4 - \lambda^4)^2}\left\{(\lambda_1^4 + \lambda^4)C_1' + 2\lambda^2 C_1'''\right\} + B_1\left\{b_1\frac{\cosh\lambda y}{\cosh \tfrac{1}{2}\lambda} - \frac{2y}{\mu_1^4 - \lambda^4}(\lambda^2 S_1 + S_1'') + \frac{4}{(\mu_1^4 - \lambda^4)^2}\{(\mu_1^4 + \lambda^4)S_1' + 2\lambda^2 S_1'''\}\right\}$$

where

$$C_1 = \frac{\cosh\lambda_1 y}{\cosh \tfrac{1}{2}\lambda_1} - \frac{\cos\lambda_1 y}{\cos \tfrac{1}{2}\lambda_1}$$

$$S = \frac{\sinh\mu_1 y}{\sinh \tfrac{1}{2}\mu_1} - \frac{\sin\mu_1 y}{\sin \tfrac{1}{2}\mu_1}$$

and $\lambda = 3.98$, $\lambda_1 = 4.73$, $\mu_1 = 7.8532$, $B_1 = 0.2719$ and $'$ denotes differentiation with respect to $y$ and

$$a_1 = \frac{2\lambda_1^2}{\lambda_1^4 - \lambda^4} - \frac{16\lambda^2\lambda_1^3\tanh \tfrac{1}{2}\lambda}{(\lambda_1^4 - \lambda^4)^2}$$

$$b_1 = \frac{2\mu_1^2}{\mu_1^4 - \lambda^4} - \frac{16\lambda^2\mu_1^3\coth \tfrac{1}{2}\mu_1}{(\mu_1^4 - \lambda^4)^2}$$

We then have

$$I = \tfrac{1}{2}\rho\nu a^2 V_m^2\int_{-\frac{1}{2}}^{\frac{1}{2}} PS(1 - 4y^2)dy$$

$$= \tfrac{1}{2}\rho\nu a^2 V_m^2(41.14) \times 10^{-4}$$

$$K = -\frac{\rho\nu^3 R_i a^2}{36\lambda^2 d^3}\int_{-\frac{1}{2}}^{\frac{1}{2}}(\lambda^2 P - P'')^2 dy$$

$$= -\frac{\rho\nu^3 R_i a^2}{36\lambda^2 d^3}1\,549$$

Also

$$\frac{dV_R}{dr} - \frac{V_R}{r} = \frac{SPV_m a^2}{12d} - \frac{V_m a^2}{12d}\int_{-\frac{1}{2}}^{\frac{1}{2}} SP dy$$

so that

$$J = \frac{V_m^2 a^4 \rho\nu R_i}{72d}\left\{\left(\int SP\,dy\right)^2 - \int (SP)^2 dy\right\}$$

$$= \frac{V_m^2 a^4 \rho\nu R_i}{72d}(-48.35)10^{-6}$$

Then, returning to the energy equation and dividing through by $\tfrac{1}{2}\rho\nu V_m^2$ (constant).

$$\frac{da^2}{dt} = 0 = a^2(41.14)10^{-4} - \frac{a^4 R_i}{36d}(48.35)10^{-6} - \frac{a^2 1\,549}{\lambda^2 T}$$

If the Reynolds stress term $J$ is neglected, then we see that the critical Taylor number is given by

$$I + K = 0$$

that is

$$\lambda^2 Tc = 37.65 \times 10^4$$

or

$$Re\sqrt{\frac{d}{R_i}} = 36.34$$

which compares satisfactorily with the value of 35.94 given by Chandrasekhar. This number, $Re\sqrt{d/R_i}$, is usually known as the Dean number. The equilibrium amplitude is given by

$$a_e^2 = 3063\frac{d}{R_i}\left(1 - \frac{Tc}{T}\right)$$

We are now in a position to compare this result with the amplitude factor used by Chang and Mockros. In our notation, the formula they use is

$$u' = -\frac{\alpha\lambda}{d}P(y)\cos\gamma z$$

to compare with our

$$u' = -\frac{\nu a_e}{6d}P(y)\cos\gamma z$$

Thus we must have

$$\alpha = \frac{\gamma a_e}{6\lambda}e$$

Also

$$\alpha = \frac{\beta}{Re}\left(1 - \frac{Tc}{T}\right)^{\frac{1}{2}}$$

$$= \frac{\nu}{6\lambda}\sqrt{3\,063}\sqrt{\frac{d}{R_i}}\left(1 - \frac{Tc}{T}\right)^{\frac{1}{2}}$$

$$\beta = \frac{\nu}{6\lambda}\sqrt{3\,063}\,Re\sqrt{\frac{d}{R_i}}$$

## NOTATION: SUPPLEMENT

- $P$ = pressure
- $r$ = radial cylindrical polar coordinate
- $R_o$ = outer cylinder radius
- $U$ = velocity component in $r$ direction
- $V$ = velocity component in $\theta$ direction
- $V_o$ = unperturbed velocity
- $V_R$ = contribution to velocity from the Reynolds stress terms
- $W$ = velocity component in $z$ direction, that is, parallel to cylinder axes
- $z$ = axial cylindrical polar coordinate
- $\rho$ = density
- $\theta$ = cylindrical polar coordinate (azimuthal)
- $\gamma$ = dimensional critical wave number for disturbance

## LITERATURE CITED: SUPPLEMENT


Davey, A., "The growth of Taylor vortices in flow between rotating cylinders," *J. Fluid Mech.*, 14, 336-68 (1962).

Mori, Y., and Y. Uchida, "Forced convective heat transfer in a curved channel," *J.S.M.E.*, 1967 Semi-international Symposium, Tokyo, pp. 181-190 (1967).

Stuart, J. T., "Nonlinear stability theory," *Ann. Rev. Fluid Mech.*, 3, 347-370 (1971).



*Manuscript received June 16, 1976; revision received September 7, and accepted September 8, 1976.*